

Corrosion behavior of MgO-MgAl₂O₄-FeAl₂O₄ composite refractory materials

Tuba (Aksoy) Bahtli¹ · Cemal Aksel² · Taner Kavas³

Received: 6 May 2016 / Revised: 29 September 2016 / Accepted: 21 October 2016 / Published online: 13 January 2017
© Australian Ceramic Society 2017

Abstract This paper investigated the corrosion behavior of refractory materials that were produced by incorporating hercynite (FeAl₂O₄, H) at different ratios into MgO-MgAl₂O₄ (spinel, S). Meanwhile, the values of density and open porosity of those samples were also measured. The corrosion resistance of those composite refractory materials was determined by measuring the penetration distances and spreading areas. The influence of corrosion resistance based on the microstructural changes occurred as a result of solubility of constituents in the interface of clinker-refractory for different regions was examined by using SEM. The incorporation of FeAl₂O₄ into MgO-MgAl₂O₄ decreased the porosity of composite refractory materials and also reduced the penetration distances and spreading area values of the corroded regions of refractories, leading to improvement on the corrosion resistance. The optimum amounts of constituents incorporated into new composite refractory materials used for obtaining longer service life in industrial applications were determined.

Keywords MgO · MgAl₂O₄ · FeAl₂O₄ · Refractory · Corrosion

Introduction

The chrome-free bricks have taken the place instead of magnesia-chrome brick used in the sintering zone of the cement rotary kiln with the increase of cement technology development and the importance of environmental protection. Cr (VI) has been associated with allergic skin ulceration and carcinomas in humans, diffuses from refractory into the cement clinker, and increases the risk of toxic reactions during processing of cement. In this sense, the research efforts, in general, are on the development of magnesia-spinel (MgO-MgAl₂O₄), dolomite, and magnesia-zirconia bricks [1].

MgO-spinel bricks are widely used at transition regions of the cement rotary kilns due to their wear resistance and thermal shock resistance. MgO-spinel bricks have also sufficient corrosion resistance and high thermal conductivity [2].

In recent years, as an alternative to MgO-chrome brick, the production of MgO-hercynite bricks is also accelerating like MgO-spinel. In general, hercynite production commercially is carried out by solid-state reaction of oxides at high temperatures and prolonged period (such as 16 h) under a relatively low oxygen pressure controlled atmosphere [3].

New research has shown that magnesia-hercynite bricks show superior performance in terms of coating and flexibility features [2]. Fe₂O₃ and Al₂O₃, take place as a component of CaO-Al₂O₃-Fe₂O₃ system, such as C₄AF and C₂F, enhance the coatibility of cement materials. The better the stability of the coating is obtained due to diffusion of Fe₂O₃ in the reaction zone. Based on the cement clinker resistance test carried out at 1500 °C, magnesia-chrome brick is severely affected by

✉ Tuba (Aksoy) Bahtli
taksoy@konya.edu.tr

¹ Engineering and Architecture Faculty, Department Of Metallurgical and Materials Engineering, Necmettin Erbakan University, Konya, Turkey

² Engineering Faculty, Department of Materials Science and Engineering, Anadolu University, Eskisehir, Turkey

³ Engineering Faculty, Department of Materials Science and Engineering, Afyon Kocatepe University, Afyon, Turkey

clinker, but magnesia and magnesia-spinel-hercynite bricks displayed higher corrosion resistance [4].

Corrosion can be considered as the debonding and subsequent physical fragmentation of the refractory, due to destruction of the bond liquid glass, together with the chemical dissolution of all phases [5].

In this study, the corrosion resistance and therefore the service life of bricks are intended to increase by combining the advantages of $MgAl_2O_4$ and $FeAl_2O_4$ and determining the optimum chemical composition with the addition of hercynite at different ratios to MgO-spinel.

Methods and procedures

Recipes were prepared by incorporating with 5, 10, and 20% hercynite (H) to the compositions obtained by additions of 5, 10, and 20% $MgAl_2O_4$ spinel (S) by weight to MgO (M). Raw materials were weighed according to recipes; binder solutions as 1% by weight of $MgSO_4$ and 1% totanin (93% MgO and Al_2O_3 , Fe_2O_3 , SiO_2 , CaO) were added and were prepared, blended by stirring for 10 min. The press pressures applied for cylindrical and square-shaped specimens were therefore ~ 175 and ~ 35 MPa, respectively. The sintering temperature of all samples was ~ 1600 °C, and dwelling time at maximum temperature was about ≥ 10 h. Three parts were cut for each material prepared in different compositions; these pieces were boiled in the water for 2 h and cooled to room temperature. Thus, removal of the air in pores and pores filled with water was provided. Then, density and open porosity values were determined by Archimedes principles.

According to standards, corrosion tests were performed in two ways in order to determine the interaction of the cement clinker with MgO-based composite refractory materials that contain different additive components in different proportions:

1. In the first one, samples were prepared 50 mm \times 50 mm \times 50 mm square prism form; the hole (diameter ~ 18 mm, depth ~ 20 mm) was drilled on top of them. Then, 8-g ($D_{100} < 63$ μm) cement clinker/slag was put into those holes; static corrosion tests were performed in the furnace (Nabertherm HT16/18) using 10 °C/min of heating and cooling rates where the dwelling time was 72 h at 1500 °C.

The refractory samples had been cut into half by a diamond disc 1.5-mm thick in order to examine the cross-sectional area where clinker penetrated into refractory. The dimensions of the corroded area: penetration distance “*i*” (the length of clinker infiltrating into refractories), depth of hole “*d*,” and width “*w*” values, were identified sensitively by measuring with a “digital measuring microscope” (Mahr GmbH, Model: WMS) (Fig. 1).

Samples were cut to size for coarse and fine polishing, and then cold molded by resin. The surfaces were manually polished nearly 2 min by 320-, 800-, and 1200-grit

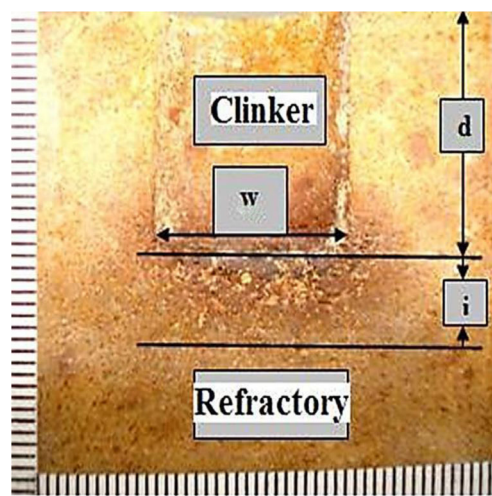


Fig. 1 The measured dimensions of corroded area at the clinker-refractory interface: *i* is the penetration distance, *d* is the depth and *w* is the width

sandpapers. Then, the polishing process was carried out nearly 15 min in Struers automatic polishing machine by using Piano 220, Largo, Dac, and Nap polishing discs.

Those samples were coated with gold-palladium alloy for 30 s. Then, in the corroded areas of refractory materials, clinker-refractory interface, microstructural changes were examined in detail by backscattered electron imaging in a scanning electron microscope (Zeiss sympathetic Evo 50) by 20-kV voltage in the regions including the following: (i) region where clinker started to penetrate into refractories (close to clinker: zone 1), (ii) the middle region between the clinker and refractory (zone 2), and (iii) the region where clinker penetration into refractories was finished (close to refractory: zone 3).

Resolutions of the different components in the clinker-refractory interface were evaluated by scanning electron microscopy with energy-dispersive X-ray analysis (SEM-EDX) of different regions. The influence of microstructural changes, which might occur with the resolution of the different components in the clinker-refractory interface, affecting the corrosion resistance was investigated.

2. Secondly, refractory materials in the form of a 10 \times 10-cm² square were prepared. Four grams ($D_{100} < 63$ μm) cement clinkers were placed at the center of sample surfaces in order to determine the amount of cement clinker spreading on the refractory surfaces. Then, the static corrosion tests were conducted at 1500 °C for 72 h with 10 °C/min heating and cooling rates. Spreading area measurements were carried out by the ImageJ program [6]. Spreading/wetting areas created on refractory materials by cement clinker were identified and examined in terms of corrosion resistance.

The chemical compositions of the cement clinker used in this study obtained by XRF chemical analysis are given in Table 1.

Table 1 Chemical compositions of cement clinker (wt. %)

Chemical compositions	Percent
K ₂ O	1.02
MgO	1.23
CaO	68.97
Al ₂ O ₃	5.50
SiO ₂	20.20
Fe ₂ O ₃	3.08
Total	100.00
Loss on ignition	1.90

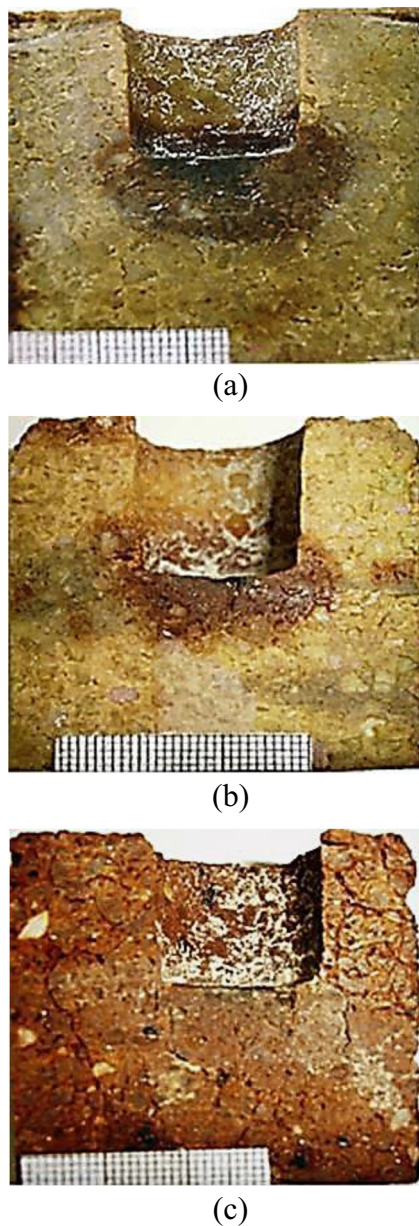


Fig. 2 Corroded refractory containing a) MgO, b) M-10S, and c) M-5S-5H that were prepared in square-prism form (scale 1 mm—the size of the smallest squares)

Results and discussion

Corroded model samples are given in Fig. 2. It showed that the amount of penetration of cement clinker into refractory decreased with the addition of both spinel to MgO and the addition of hercynite to MgO-spinel.

Density and open porosity results of MgO-spinel (M-S) and MgO-spinel-hercynite (M-S-H) composite materials produced by adding additives in varying ratios are given in Fig. 3.

Density values in all materials produced increased while the open porosity values of them decreased. In general, MgO-spinel-hercynite composites have higher density and lower open porosity values than MgO-spinel materials. In addition, density values also decreased as the amount of additives increased. The highest density value was achieved in M-5%S-5%H material (Fig. 3).

The changes in penetration distance, depth and width values of clinker depending on the amount of additives in regions where the refractory materials were corroded are shown in Fig. 4. M-5%S-H, M-10%S-5%H, and M-10%S-20%H composite materials show in general lower penetration distances than M-S refractories.

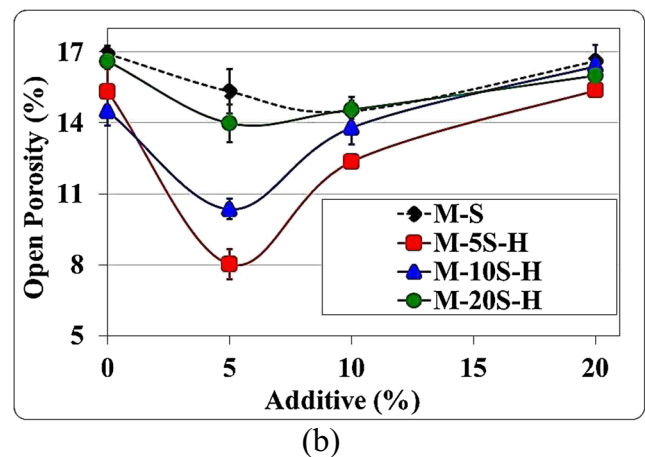
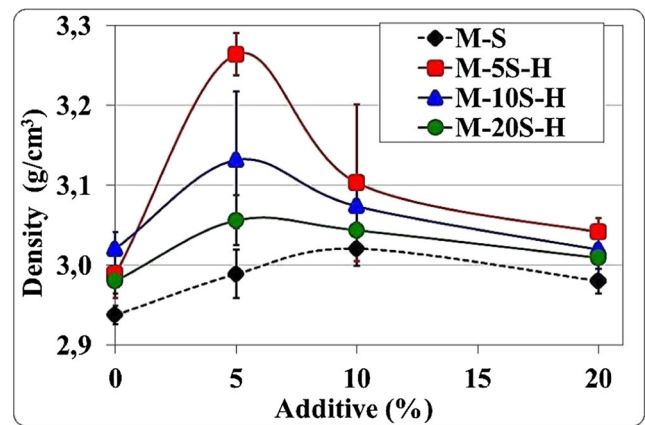
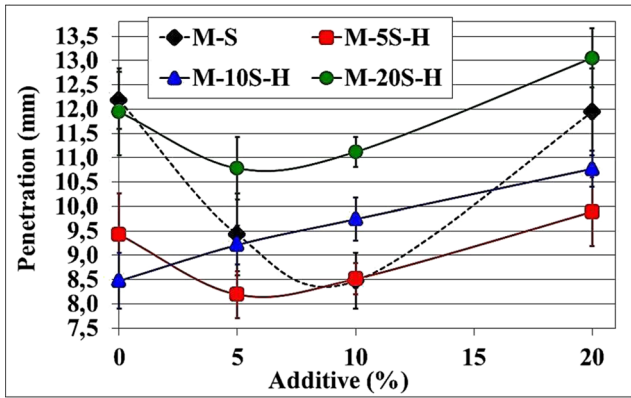


Fig. 3 a) Density and b) open porosity values of composite materials as a function of additives

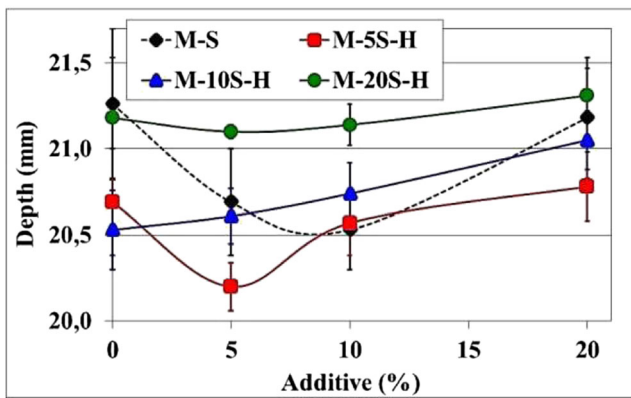
Furthermore, penetration of clinker into the refractory took place at the minimum level in M-5%S-5%H refractory that has the highest density and the lowest porosity, where the improvement achieved was approximately 13% compared to M-5%S material. In general, as porosity decreased, the penetration distances of clinker into the refractory were also decreased. The decrease in porosity with increasing density as a result of filling pores with additives led to increase in

corrosion resistance, and therefore it is concluded that porosity is an important parameter affecting corrosion resistance.

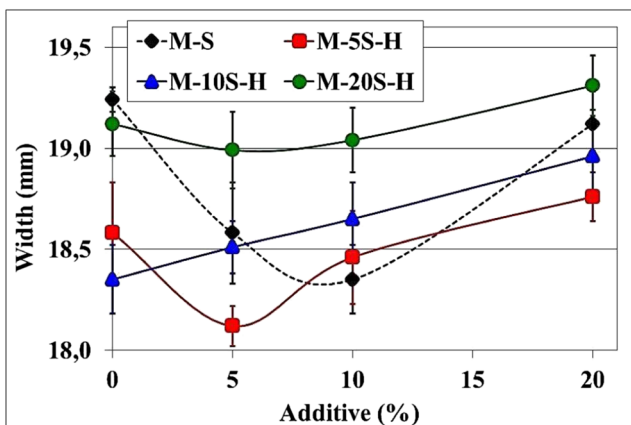
Depth and width values of holes filled with clinker were drilled on the top of the corroded composite refractories that



(a)

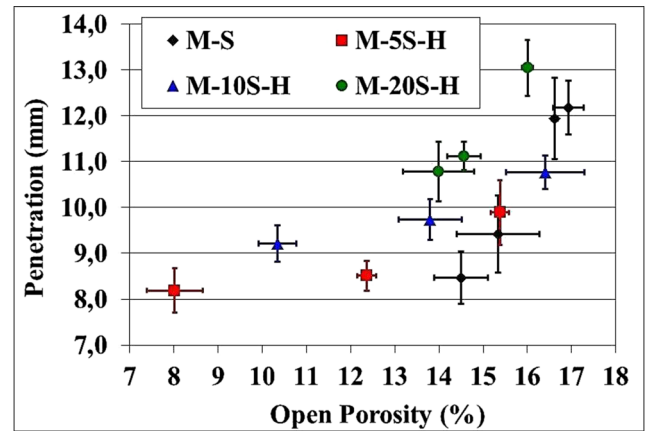


(b)

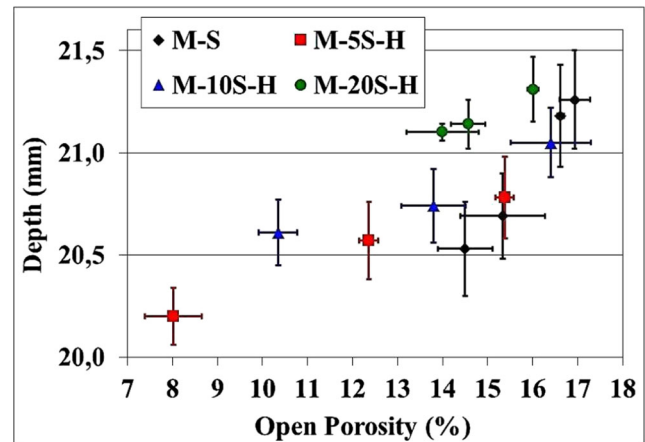


(c)

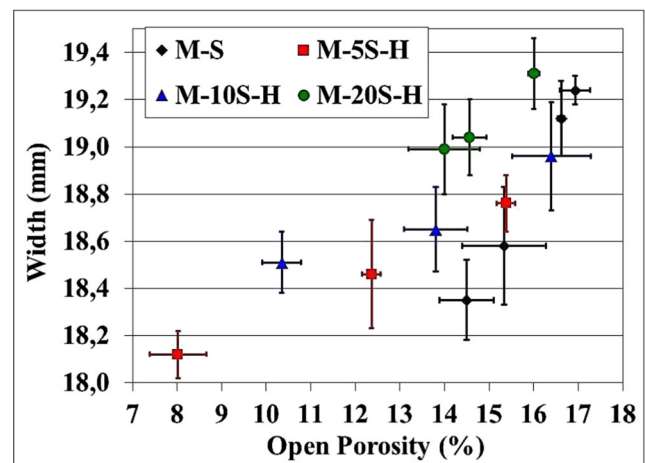
Fig. 4 a) Penetration, b) depth, and c) the width distance values of clinker as a function of additives



(a)



(b)



(c)

Fig. 5 a) Penetration distance, b) depth, and c) the width values of clinker for M-S and M-S-H composite refractory materials as a function of open porosity

Fig. 6 **a**) Backscattered electron (BSE) image of zone 1 of corroded M-5%S-5%H refractory material ($\times 500$). **b** and **c**) Microstructural image and colorized BSE image of zone 1 of corroded M-5%S-5%H refractory material. **d–h**) The element distributions of zone 1 of corroded M-5%S-5%H refractory material (**d** Mg, **e** Al, **f** Fe, **g** Ca, **h** Si)

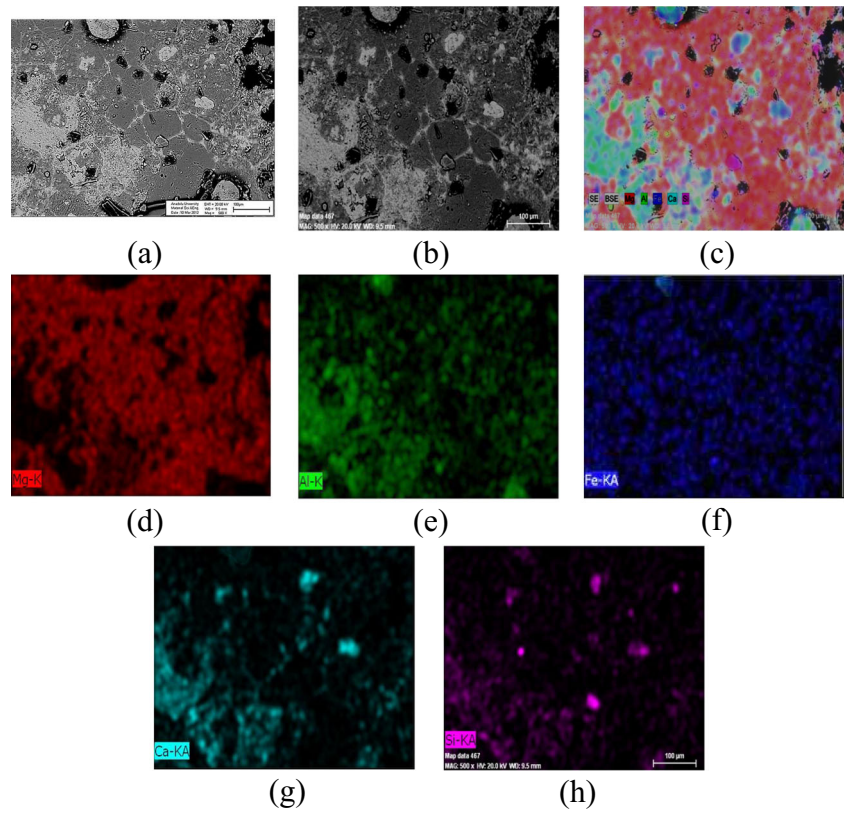


Fig. 7 **a**) BSE image of zone 2 of corroded M-5%S-5%H refractory material ($\times 500$). **b** and **c**) Microstructural image and colorized BSE image of zone 2 of corroded M-5%S-5%H refractory material. **d–h**) The element distributions of zone 2 of corroded M-5%S-5%H refractory material (**d** Mg, **e** Al, **f** Fe, **g** Ca, **h** Si)

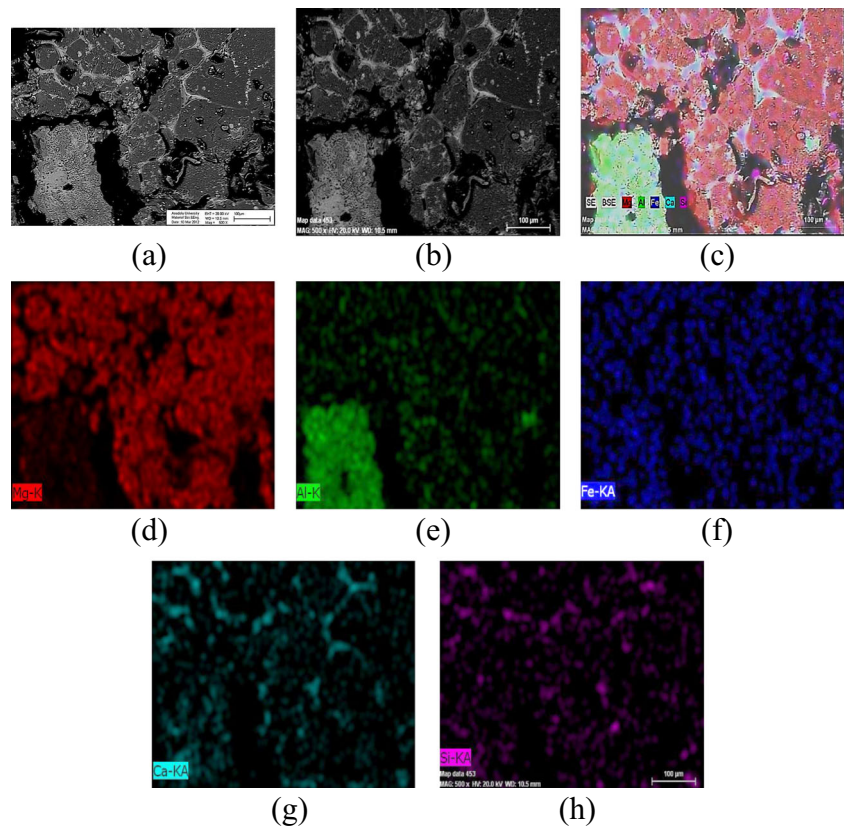
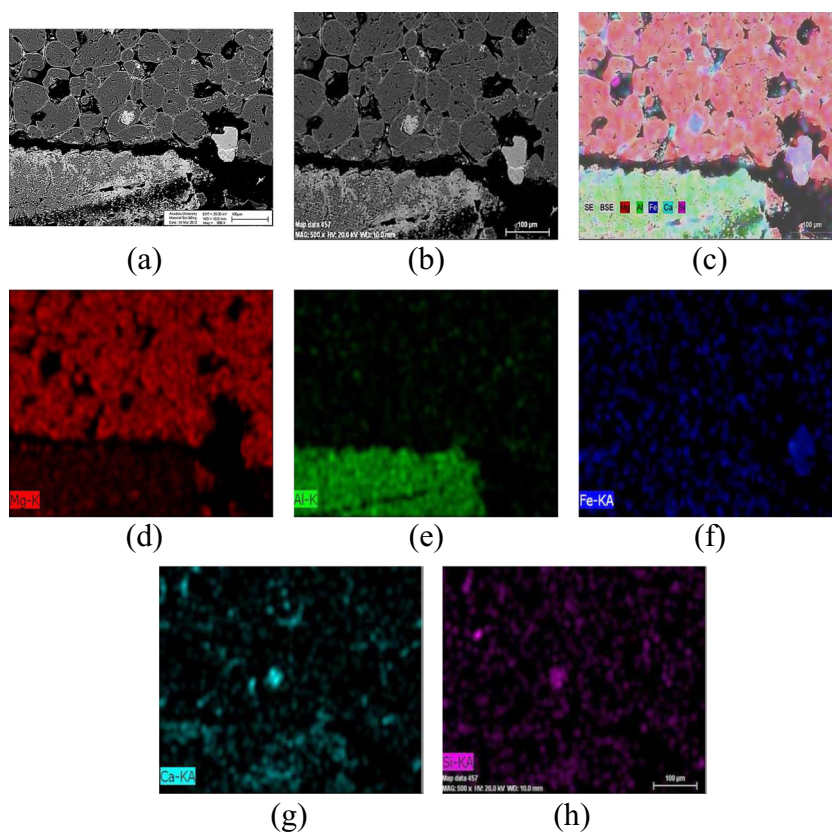


Fig. 8 **a)** BSE image of zone 3 of corroded M-5%S-5%H refractory material ($\times 500$). **b** and **c)** Microstructural image and colorized BSE image of zone 3 of corroded M-5%S-5%H refractory material. **d–h)** The element distributions of zone 3 of corroded M-5%S-5%H refractory material (**d** Mg, **e** Al, **f** Fe, **g** Ca, **h** Si)



produced by adding spinel and hercynite at different ratios are given respectively in Fig. 4b, c.

In general, smaller depth and width formed in M-5%S-H and M-10%S-H composite materials than in M-5%S and M-10%S composite refractories, which means less interaction between clinker and those materials occurred leading to less wear and less area loss in the corroded regions. For example, compared with the M-5%S material, hercynite addition to those materials substantially increases the corrosion resistance.

It is observed that M-5%S-5%H composition that has the lowest penetration distance, has also the lowest depth and the

lowest width values. It was concluded that the amount of the penetration depth and width values authenticate each other.

Penetration, depth, and width values as a function of the amount of open porosity of clinker-refractory interfaces for M-S and M-S-H materials are respectively shown in Fig. 5.

In general, as the amount of pores decreased in M-S refractories produced by addition of hercynite in varying proportions, it was determined that the penetration distance, depth, and width values on clinker-refractory interface decreased as well. It is determined that M-5%S-5%H material, which has

Table 2 EDX analysis of the zone 1 in the corroded area close to the clinker in MgO-5%spinel-5%hercynite refractory material

Element	Percent	Compound	Percent
Mg	45.20	MgO	73.63
Al	5.96	Al ₂ O ₃	11.27
Si	1.34	SiO ₂	2.86
Ca	3.73	CaO	6.02
Fe	4.35	Fe ₂ O ₃	6.22
O	39.42	O	0.00
Total	100.00		100.00

Table 3 EDX analysis of the zone 2 in the corroded area between the clinker and refractory in MgO-5%spinel-5%hercynite refractory material

Element	Percent	Compound	Percent
Mg	45.20	MgO	74.95
Al	7.08	Al ₂ O ₃	13.38
Si	0.96	SiO ₂	2.06
Ca	3.11	CaO	4.35
Fe	3.68	Fe ₂ O ₃	5.26
O	39.97	O	0.00
Total	100.00		100.00

Table 4 EDX analysis of the zone 3 in the corroded area close to the refractory in MgO-5%spinel-5%hercynite refractory material

Element	Percent	Compound	Percent
Mg	45.16	MgO	74.88
Al	7.01	Al ₂ O ₃	15.02
Si	0.71	SiO ₂	1.52
Ca	2.30	CaO	3.22
Fe	4.35	Fe ₂ O ₃	5.36
O	40.48	O	0.00
Total	100.00		100.00

the highest density and the lowest amount of open porosity, has minimum clinker penetration distance.

The microstructural characterization and EDX analysis with a scanning electron microscope (SEM) of M-S-H materials were carried out to search effective parameters on the corrosion behaviors of them.

Microstructural images and also available element distributions of corroded square prism-formed MgO-5%spinel-5%hercynite composite refractory material are given in Figs. 6, 7, and 8, and the EDX analysis results are given in Tables 2, 3, and 4.

When the microstructural changes were examined, pores were identified within the grains and at grain boundaries. Gray-color spinel and lighter gray-color hercynite particles with various sizes were present on the surface of coarse MgO grains with dark gray color and at grain boundaries. Clinker penetration located intensively at grain boundaries and also at MgO grains of ternary compositions. It was observed that the cement clinker penetration into MgO particles is more pronounced where the penetration started, and decreased closer to refractory region (Figs. 6 and 7). MgO grains are relatively smaller due to cement clinker dissolution in the grain predominantly and white area contained clinker and dissolution of larger areas was more intensively observed. Small particle size can speed the process, the liquid-phase penetration, and the corrosion (Figs. 6 and 7).

Cement clinker used in this test forms the liquid phase at 1500 °C. The liquid phase filled the open pores and grain boundaries and caused abrasion. Hercynite and spinel grains also acted as a barrier for avoiding/reducing penetration even though there were small MgO grains observed, as seen in Fig. 8.

EDX analysis results in Tables 2, 3, and 4 showed that the amount of CaO decreased from the interaction region where corrosion began to the refractory region where penetration finished. As a result, penetration decreases significantly while approaching to refractory from clinker. Microstructural characterization and EDX analysis results confirmed with (i) the

penetration distance values of the cement clinker and measured (ii) depth and (iii) width values of holes.

In addition, corrosion tests were also applied to 10 × 10-cm² samples, clinker spreading areas were determined, and the sample specimens are given in Fig. 9.

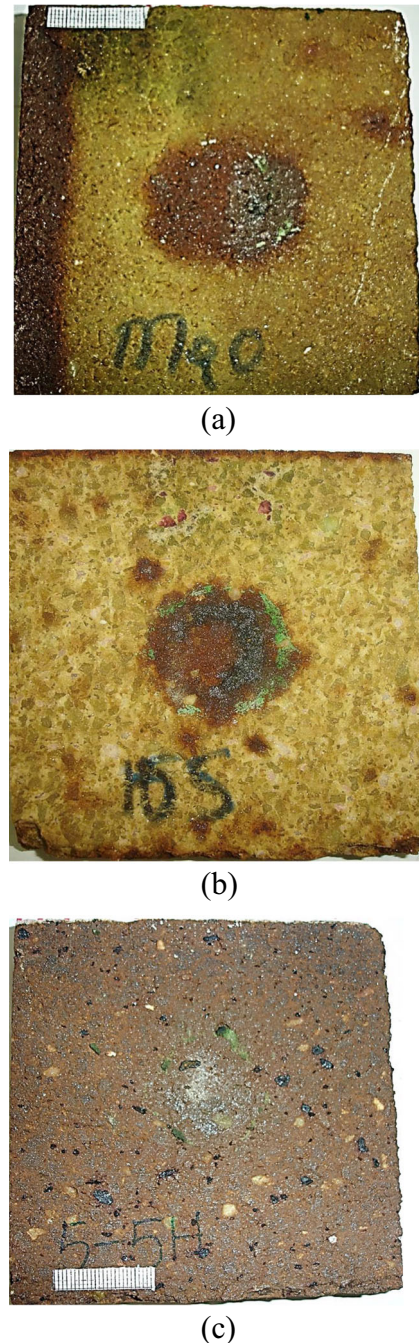


Fig. 9 Corroded refractory materials: **a**) MgO, **b**) M-10%S, and **c**) M-5%S-5%H prepared in square form (scale 1 mm—total length 10 cm)

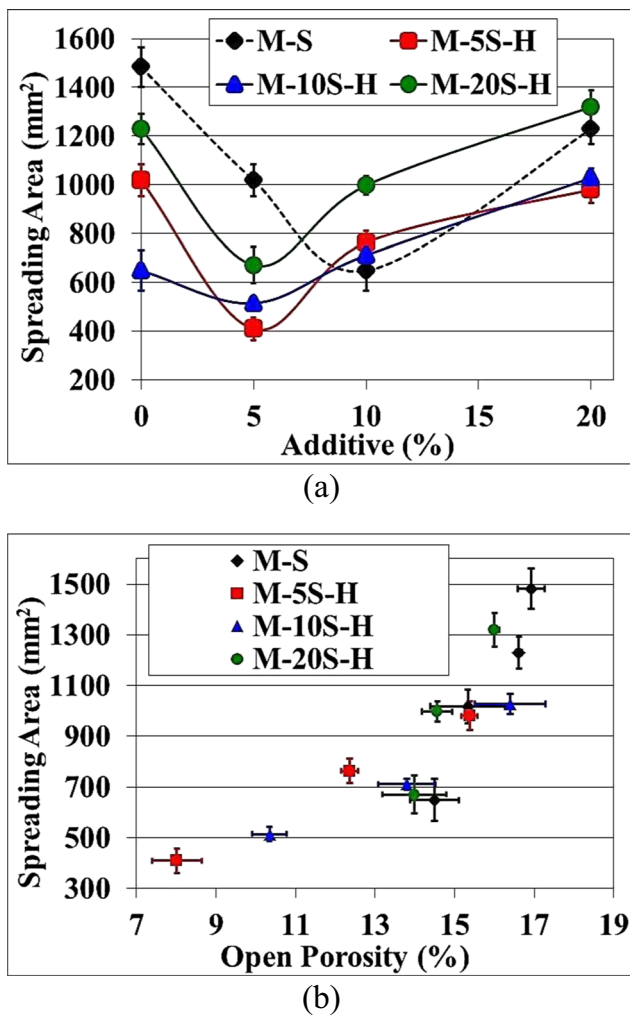


Fig. 10 Spreading areas of clinker on the surfaces of refractories as a function of **a)** the amount of additives and **b)** the amount of open porosity

The spreading area values of clinker on the surface of M-S and M-S-H materials as a function of the amount of additives and the amount of porosities are given in Fig. 10.

In general, M-S-H materials produced by 5 and 20% hercynite addition into M-S materials including 5%S and 10%S have smaller spreading area than MS materials; other M-S-H materials have bigger spreading area than M-S materials.

In general, spreading area decreased while the amount of open porosities decreased. M-5%S-5%H material has also the smallest spreading area, and improvement was achieved approximately 2.5 times compared to M-5%S material. It was determined that porosity is an important parameter affecting the corrosion resistance.

Conclusions

M-5%S-5%H material has the highest density, the lowest porosity, the smallest penetration distance, depth, and width values, and the smallest spreading area. The decrease in porosity with increasing density as a result of filling pores with additives led to increase in corrosion resistance, and therefore it is concluded that porosity is an important parameter affecting corrosion resistance. Small particle size can speed the process, the liquid-phase penetration, and the corrosion. Hercynite and spinel grains also acted as a barrier for avoiding/reducing penetration even though there were small MgO grains observed.

Acknowledgements This study was partly supported by TUBITAK under project no: 106M394. The author would like to thank Konya Selcuklu Krom Magnezit Tugla Sanayi A.S and all employees and personnel involved in this project for their support.

References

1. Aksel, C., Warren, P.D., Riley, F.L.: Magnesia-spinel microcomposites. *Journal of European Ceramic Society*. **24**, 3119–3128 (2004)
2. Ma, S., Li, Y., Sun, J., Li, Y., Xia, W.: Preparation and properties of MgO-MgAl₂O₄-FeAl₂O₄ bricks in cement kiln. *Adv Mater Res*. **250**(25), 554–560 (2011)
3. Pablo M. Botta, Estaban F. Aglietti, José M. Porto López, “Mechanochemical synthesis of hercynite”, *Mater Chem Phys*, (2002), 76, 104–109.
4. Huillin, L.: Properties of magnesia-hercynite brick. *China's Refractories*. **17**(1), 26–28 (2008)
5. Aksel, C., Riley, F.L., Konieczn, F.: The corrosion resistance of alumina-mullite-zircon refractories. *Key Engineering Materials Vols. 264-268*, 1803–1806 (2004)
6. <http://www.ansci.wisc.edu/equine/parrish/index.html>